https://doi.org/10.31925/farmacia.2026.1.14 **ORIGINAL ARTICLE**

LABISIA PUMILA (KACIP FATIMAH) PREVENTED MULTIPLE ORGAN DETERIORATIONS IN DIABETIC RATS

NAZMUN NAHAR [1,3], SUHAILA MOHAMED [1], NOORDIN MOHAMED MUSTAPHA [2], LAU SENG FONG [2], NUR ILIYANI MOHD ISHAK [1], GHADEER M. ALBADRANI [4], AMANY A. SAYED [5], MOHAMED M. ABDEL-DAIM [6,7], ABUL KALAM AZAD [8]*

[1]*Institute of Bioscience, Universiti Putra Malaysia, UPM Serdang, Malaysia*
[2]*Faculty of Veterinary Medicine, Universiti Putra Malaysia, UPM Serdang, Malaysia*
[3]*Department of Pharmacy, Faculty of Basic Medical and Pharmaceutical Science, University of Science and Technology, Chittagong*
[4]*Department of Biology, College of Science, Princess Nourah bint Abdulrahman University, P.O. Box 84428, Riyadh 11671, Saudi Arabia*
[5]*Zoology Department, Faculty of Science, Cairo University, Giza 12613, Egypt*
[6]*Department of Pharmaceutical Sciences, Pharmacy Program, Batterjee Medical College, P.O. Box 6231, Jeddah 21442, Saudi Arabia*
[7]*Pharmacology Department, Faculty of Veterinary Medicine, Suez Canal University, Ismailia 41522, Egypt*
[8]*FDepartment of Pharmaceutical Technology, Faculty of Pharmacy, University MAIWP International, Batu Caves, 6800 Kuala Lumpur, Malaysia*

**corresponding author: drazad@unimaiwp.edu.my*

Manuscript received: November 2025

Abstract

Labisia pumila (LP) is traditionally used in Malaysia for women's health. This study evaluated the protective effects of LP leaf extract on internal organs in streptozotocin (STZ)-induced diabetic rats. Thirty male rats were divided into five groups: healthy control, non-treated diabetic, diabetic treated with metformin (200 mg/kg), and diabetic treated with LP extract at 150 or 300 mg/kg. Diabetes was induced by a single intraperitoneal injection of STZ (60 mg/kg) and confirmed after 72 hours. Treatments were administered orally for 10 weeks. Serum oxidative stress, inflammatory, and epithelial biomarkers were quantified using ELISA. Untreated diabetic rats showed significantly reduced glutathione (GSH), Claudin-1, and albumin levels, along with elevated malondialdehyde (MDA), matrix metalloproteinase-13 (MMP-13), vascular endothelial growth factor (VEGF), tumor necrosis factor-α (TNF-α), and prostaglandin E2 (PGE2) compared with healthy controls. LP extract markedly attenuated diabetes-induced damage in the pancreas, liver, kidneys, heart, lungs, and spleen, and was more effective than metformin. The 150 mg/kg dose was superior at reducing oxidative stress, while the 300 mg/kg dose exerted stronger anti-inflammatory and epithelial barrier-restoring effects, indicating complementary, dose-specific actions..

Rezumat

Acest studiu a evaluat efectele extractului din frunze de *Labisia pumila* (LP) într-un model murin de diabet indus cu streptozotocină (STZ). Treizeci de șobolani masculi au fost repartizați în cinci grupuri: control sănătos, diabetici netratați, diabetici tratați cu metformin (200 mg/kg) și diabetici tratați cu extract de LP în doză de 150 sau 300 mg/kg. Diabetul a fost indus printr-o singură injecție intraperitoneală de STZ (60 mg/kg) și confirmat după 72 de ore. Tratamentele au fost administrate oral timp de 10 săptămâni. Biomarkerii serici ai stresului oxidativ, inflamației și integrității epiteliale au fost cuantificați prin metoda ELISA. Șobolanii diabetici netratați au prezentat niveluri semnificativ reduse de glutation (GSH), claudină-1 și albumină, concomitent cu creșteri ale malondialdehidei (MDA), metaloproteinazei matriceale-13 (MMP-13), factorului de creștere endotelial vascular (VEGF), factorului de necroză tumorală-α (TNF-α) și prostaglandinei E_2 (PGE_2), comparativ cu grupul de control sănătos. Extractul de LP a atenuat semnificativ leziunile induse de diabet la nivelul pancreasului, ficatului, rinichilor, inimii, plămânilor și splinei și s-a dovedit mai eficient decât metforminul. Doza de 150 mg/kg a fost superioară în reducerea stresului oxidativ, în timp ce doza de 300 mg/kg a exercitat efecte mai puternice antiinflamatoare și de restaurare a barierei epiteliale, sugerând mecanisme complementare, dependente de doză.

Keywords: streptozotocin, diabetes mellitus, *Labisia pumila* extract, metformin, internal organs

Introduction

Diabetes mellitus (DM) affects approximately 285 million people worldwide, and this number is projected to double by 2030 (1). Type 2 diabetes mellitus (T2DM), characterized by persistent high blood sugar and insulin ineffectiveness, disrupts carbohydrate, lipid, and protein metabolisms and ultimately harms multiple organs and tissues (2). The current therapeutic agents used to treat T2DM include sulfonylureas, biguanides, α-glucosidase

inhibitors, and thiazolidinediones. These drugs are fraught with undesirable side effects and, on prolonged use, will cause a decrease in response (2). DM can cause a range of serious complications affecting various body organs, such as neuropathy, nephropathy, retinopathy, cardiovascular disease, stroke, and gangrene (3). DM also adversely affects the respiratory, digestive, genitourinary, and central nervous system (CNS) (4). Currently, there are very few reports on the use of therapeutics to minimize T2DM-related internal organ abnormalities. Metformin is a primary treatment used as a first-line hypoglycemic agent for people with diabetes mellitus. Metformin, through its anti-inflammatory effects on AMPK-dependent and AMPK-independent pathways and antioxidative properties, protects against endotoxin-induced fulminant hepatitis in mice (5). Metformin may induce heartburn, abdominal pain, nausea, emesis, bloating, diarrhea, constipation, and weight reduction. LP (*Primulaceae*), known as Kacip Fatimah in Malaysia, is a rainforest herb of Southeast Asia that is especially rich in gallic acid and myricetin with alleged anti-aging properties (6). The LP is rich in various phenolic compounds, including flavonoids, gallic acid, quercetin, myricetin, kaempferol, and catechin. The phytochemicals found in LP include ascorbic acid, tocopherols, β-carotene, and other carotenoids, which exhibit anti-oxidant, free-radical scavenging, and anti-inflammatory properties (7). This research demonstrated the safety and effectiveness of LP leaf extract in managing diabetes in rats. This study established the safety and efficacy of LP leaf extract in treating diabetes in rats. The histopathological changes in the vital organs determined the safety and efficacy of the LP leaf extract. The safety and efficacy of the LP leaf extract were determined by histopathological examination of vital organs.

Materials and Methods

Preparation of LP extract

LP leaves (Herbagus Trading, Penang, Malaysia) were dried and milled, then extracted with 10 times their weight of 50% aqueous ethanol under mechanical shaking at room temperature for 72 hours. The extract was subjected to rotary evaporation and then dried in an oven at 35°C. The LP extract is first frozen to a very low temperature, such as -40°C. After creating a low-pressure condition by evacuating and adding a small amount of heat, the ice sublimates directly into vapor and is collected in a condenser. The extraction yield of 0.322% was calculated based on the final extract weight of 8.7 grams relative to the weight of the 2.7 kg powder after drying. Sample extracts from LP were stored at 4°C in a refrigerator, and additional samples were taken as needed for testing. The HPLC profile indicates that the LP extract predominantly comprises gallic acid and myricetin (8, 9).

Animals

Male Sprague-Dawley (A-Sapphire Enterprise, Seri Kembangan, Malaysia) rats weighing 200 ± 20 g, that were nine weeks old and randomly assigned to polypropylene cages (two rats per cage), with bedding material of wood shavings, were kept at 27 ± 2°C, 55 ± 10% relative humidity, and a 12-hour light/dark cycle. In addition, they were given complimentary access to water and rat food, which included Gold Coin and Klang varieties from Malaysia. The experimental techniques were approved by Prof. Dr. Mohd Hair Bejo, Chairman of the Universiti Putra Malaysia Institutional Animal Care and Use Committee, on 7th February 2018 under protocol UPM/IACUC/AUP-R095/2017. At the Animal House, which is part of the Faculty of Medicine and Health Sciences at University Putra Malaysia, six rats were allocated into five different groups (n = 6): a healthy control group, a group with induced diabetes through STZ receiving no treatment, and diabetes groups treated with either 200 mg/kg of body weight metformin, 150 mg/kg or 300 mg/kg of body weight of LP leaf extract. The acclimatization period spans weeks 1. STZ was administered at 60 mg/kg body weight in a freshly prepared solution in 0.9% NaCl, pH 5.6, and kept on ice to maintain stability; 2 µL of this solution was injected immediately after preparation to ensure potency. Week 2 diabetes induction was achieved *via* intraperitoneally injection of STZ (Sigma Chemical Co., St. Louis, MO, USA) at a dose of 60 mg/Kg. Diabetes onset was confirmed by a fasting blood glucose level exceeding 11.1 mmol/L measured 72 hours after STZ treatment (10). The treatment phase occurs between weeks 4 and 13. The treatments administered were: Metformin at 200 mg/kg, LP at 150 mg/Kg and 300 mg/Kg (11), and oral gavage treatment commenced 10 weeks following diabetes induction and was administered continuously until sacrifice. The required daily dose for a 200g rat to achieve dosage rates of LP 150 mg/kg/day, 300 mg/kg/day, and metformin 200 mg/kg/day was calculated using the formula: D = R \Weight, resulting in total daily doses of 30 mg, 60 mg, and 40 mg, respectively. The fasting blood glucose concentration measured after a 12-hour fast was determined using an AccuCheck Performa glucometer (USA), Roche Diabetes Care (Product Code: ACHKPRFM1) from blood samples obtained by tail-vein puncture at weeks 3, 5, 11, and 13. At week 13, the animals were sacrificed, and blood samples were collected for analysis. Rats were administered insulin subcutaneously at a dosage of (4 IU/200 g/day) if their blood glucose concentration surpassed 32 mmol/L (12), (Figure 1).

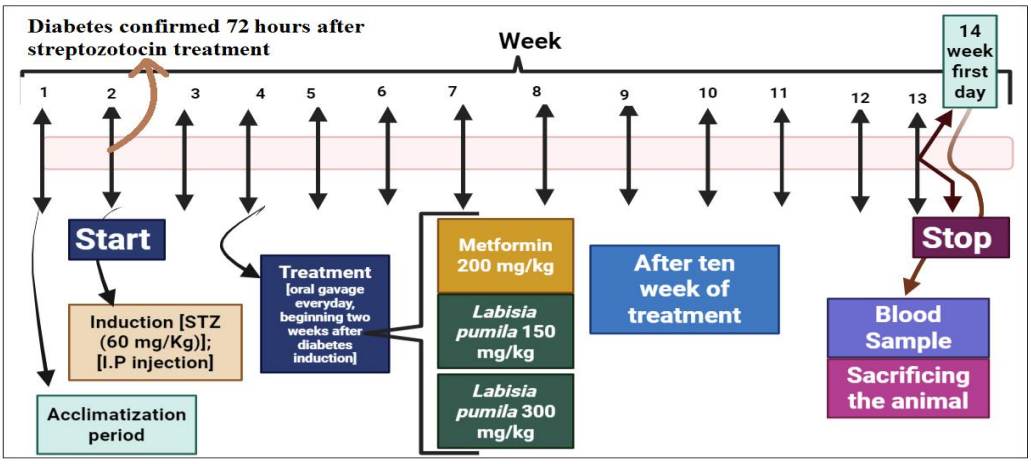

Figure 1.
The time-point schedule for the animal study

Organ somatic index (organ weight/body weight %)
After ten weeks of therapy, the rats were exsanguinated under intraperitoneal anesthesia with a combination of xylazine (10 mg/kg), atropine (0.15 mg/kg), and ketamine hydrochloride (50 mg/kg). Blood samples centrifuged at 300 × g were used to extract serum. We collected, rinsed with ice-cold saline, dried, and weighed the liver, spleen, heart, lungs, and kidneys. Each animal's Organ Somatic Index (OSI) was calculated by dividing its organ weight by its body weight.

Histopathology and Histology Scoring
The liver, heart, lungs, kidneys, spleen, and pancreas were harvested and fixed in 10% neutral-buffered formalin for 24 hours at a minimum fixative-to-tissue volume ratio of 10:1 (volume/ volume) to ensure adequate fixation and preservation of morphology. Tissues were subsequently processed through dehydration using graded ethanol (70%, 95%, and 100%, cleared with xylene, and infiltrated/embedded in molten paraffin wax at 60-62°C under vacuum. The resulting paraffin blocks were sectioned at 4 µm.

For staining, sections were deparaffinized in xylene and rehydrated through graded ethanol. Nuclei were stained using Harris Hematoxylin for 5 minutes, followed by a brief differentiation in 1% acid alcohol and bluing in Scott's tap water substitute. Cytoplasm and matrix were counterstained with 5% aqueous Eosin Y for 30 seconds. Following dehydration and clearing in xylene, sections were mounted and inspected under a light microscope for histological alterations. Microscopic images were acquired using a Motic BA410 light microscope connected to a Moticam Pro 285A digital camera. All image capture, morphometric measurements, and analysis were performed utilizing the dedicated image analysis software, Motic Images Plus 2.0 ML (Faculty of Veterinary Medicine, Universiti Putra Malaysia, UPM). All microscopic observations and morphometric analyses were conducted at a total magnification of 400X (using the 40X objective lens and the 10X ocular lens).

Pancreas and Liver Histology Scoring
For pancreas (islets), the scoring method is: Islet morphology was graded on a four-point scale (0–3), where 0 indicates normal islets with intact architecture, 1 denotes mild alterations such as slight vacuolization or minor cell loss, 2 reflects moderate degeneration with partial vacuolization, and 3 represents severe islet destruction characterized by necrosis or extensive cellular loss. Liver injury was evaluated using a semi-quantitative scoring system based on two histological parameters: hepatocyte degeneration/ necrosis and sinusoidal and vascular changes. Each parameter was scored on a scale of 0–3. Hepatocyte degeneration/necrosis was graded as follows: 0, normal hepatocytes with intact architecture; 1, mild cellular swelling and minor degeneration; 2, moderate degeneration with occasional necrotic hepatocytes; and 3, severe degeneration with widespread hepatocyte necrosis. Sinusoidal and vascular alterations were scored as 0, normal sinusoids and portal triad; 1, mild sinusoidal congestion or dilation; 2, moderate congestion with inflammatory cell infiltration; and 3, severe congestion, marked inflammation, or fibrosis (13).

Renal glomerular and Medulla Histology scoring
Glomerular Histopathological alterations were assessed using a semi-quantitative scoring system based on five parameters: glomerular damage, tubular necrosis, tubular vacuolization, interstitial edema/hemorrhage, and glycogen deposition. Each parameter was graded on a scale of 0 to 3, with 0 indicating no renal injury and 3 indicating severe renal injury. Glomerular damage was evaluated for necrosis, shrinkage, or sclerosis and scored as 0 (normal), 1 (mild; < 25% of glomeruli affected), 2

(moderate; 25-50%), or 3 (severe; > 50%). Tubular necrosis involving proximal and/or distal tubules was scored as 0 (none), 1 (mild; < 10% of tubules affected), 2 (moderate; 10-25%), or 3 (severe; > 25%). Tubular vacuolization was graded from 0 (none) to 3 (severe) according to the extent of vacuolated tubular epithelial cells. Interstitial edema or hemorrhage in the renal cortex and medulla was scored from 0 (none) to 3 (severe). Glycogen deposition was identified as PAS-positive or vacuolated areas and graded from 0 (absent) to 3 (severe). Histological changes in the renal medulla were assessed based on four parameters: tubular necrosis, tubular vacuolization, tubular dilation/ lumen widening, and interstitial edema/hemorrhage. Tubular necrosis involving the loop of Henle, collecting ducts, and renal papillary ducts was graded as 0 (none), 1 (mild; < 10% of tubules affected), 2 (moderate; 10-25%), or 3 (severe; > 25%). Tubular vacuolization was scored from 0 (none) to 3 (severe) according to the extent of vacuolated tubular epithelial cells. Tubular dilation or lumen widening was graded on a scale of 0 (none) to 3 (severe) based on the degree of tubular distension. Interstitial edema or hemorrhage within the medullary region was similarly scored as 0 (none), 1 (mild), 2 (moderate), or 3 (severe) (14).

Heart tissues Histology scoring

Cardiac histopathological alterations were assessed using a semi-quantitative scoring system. Tissue injury was graded on a four-point scale: 0 (normal), 1 (mild), 2 (moderate), and 3 (severe). The epicardium and myocardium were evaluated independently. Epicardial changes were assessed based on structural integrity, edema or thickening, inflammatory cell infiltration, and vascular congestion or hemorrhage. Myocardial alterations were evaluated by examining myofibrillar disorganization, myocyte degeneration or necrosis, interstitial edema, and inflammatory cell infiltration (15).

Histopathological evaluation of lung tissue

Pulmonary histopathological alterations were evaluated using a standardized semi-quantitative scoring system tailored to assess structural changes in bronchioles, terminal bronchioles, alveolar regions, and pneumocytes. Tissue injury was graded on a four-point scale: 0 (normal), 1 (mild), 2 (moderate), and 3 (severe). Bronchiolar and terminal bronchiolar changes were assessed based on epithelial thickening or degeneration, luminal narrowing, peribronchiolar inflammatory cell infiltration, and smooth muscle hypertrophy. Alveolar region alterations were evaluated by examining alveolar septal thickening, alveolar space distortion or collapse, interstitial edema, and inflammatory cell infiltration. Pneumocyte-related changes were assessed based on type I pneumocyte damage, type II pneumocyte hyperplasia, and cellular degeneration or necrosis (16).

Histopathological evaluation of the spleen tissue

Splenic histopathological alterations were assessed using a semi-quantitative scoring system. Tissue changes were graded on a four-point scale: 0 (normal), 1 (mild), 2 (moderate), and 3 (severe). Evaluation was performed across four anatomical and functional compartments: splenic capsule, white pulp, red pulp, and inflammatory response. Capsular changes were assessed based on capsular thickening and structural disruption. Alterations in the white pulp, including the periarteriolar lymphoid sheath (PALS), marginal zone (MZ), follicles (FZ), and central arteriole (CA), were evaluated for PALS disorganization, marginal zone disruption, lymphoid depletion, and germinal center alterations. Red pulp pathology, involving the red pulp sinusoids (RP), blood sinuses (BS), and splenic cords (SC), was assessed by examining sinusoidal congestion, splenic cord expansion, and hemorrhage or vascular dilation. The inflammatory response was evaluated based on the extent of inflammatory cell infiltration. The scores for each parameter were recorded for all sections, and the severity of the above tissue injury was expressed as the mean histopathological score *per* experimental group, with higher scores indicating greater tissue damage (17).

Biochemical parameters

The Hitachi Clinical Analyzer (Hitachi, Japan) was used to assess serum albumin, creatinine, blood urea nitrogen (BUN), aspartate aminotransferase (AST), and alanine aminotransferase (ALT) levels. Serum concentrations of MDA, GSH, VEGF-A, PGE_2, TNF-α, claudin-1, and MMP-13 were quantified using commercial ELISA kits from Qayee Biotechnology and Elabscience Biotechnology Co., China. Serum levels of MDA, GSH, PGE_2, TNF-α, VEGF-A, and MMP-13 were quantified using commercial ELISA kits from Elabscience Biotechnology Inc. (China). The following kits were used: MDA (Cat. No. E-EL-0060), GSH (Cat. No. E-EL-0026), PGE_2 (Cat. No. E-EL-0034), TNF-α (Cat. No. E-EL-R2856), VEGF-A (Cat. No. E-EL-R2603), and MMP-13 (Cat. No. E-EL-R0045). Lot numbers were confirmed and recorded from the external kit labels, while claudin-1 was determined using the Rat Claudin-1 ELISA kit (Qayee Biotechnology; Catalogue No. QY-E10760). All kits were used according to the manufacturers' instructions, and lot numbers were recorded from the outer labels of each kit. Samples and standards were assayed in duplicate following the manufacturer's sandwich ELISA procedures, and absorbance was measured at 450 nm using a microplate reader. Serum samples were initially diluted 1:2; if the OD exceeded the highest standard (20 ng/mL), further dilutions of 1:4, 1:8, or 1:16 were used. The standard

curve was prepared by serially diluting the 20 ng/mL stock standard 1:2 to generate working standards at 10, 5, 2.5, 1.25, 0.63, 0.31, and 0 ng/mL. For the other ELISA targets, samples were diluted as recommended by the respective kit protocols to ensure readings fell within the standard curves. Measured concentrations were multiplied by the corresponding dilution factor to determine the actual concentration in the original samples. Absorbance was measured at 450 nm using a microplate reader. Sample concentrations were calculated using quadratic regression. Other ELISA samples were diluted as recommended, and final concentrations were obtained by multiplying the measured values by the respective dilution factors.

Statistical Analysis

Statistical analyses were performed using SPSS 22.0 (SPSS Inc., Illinois, USA). Significance was set at $p < 0.05$, assessed through one- or two-way ANOVA with Duncan's post hoc test. The best-fit equations for linear and quadratic regressions were generated using the MyCurveFit online tool. All results are presented as mean ± SEM.

Results and Discussion

Fasting blood glucose (FBG) and body weight

Non-treated rats with STZ-induced diabetes showed elevated ($p < 0.05$) FBG (Table I), polyuria, polydipsia, polyphagia, and fatigue. Diabetic rats treated with LP extracts or metformin did not show these clinical signs. However, FBG concentrations were high during the first 5 weeks of extract treatment and the first 11 weeks of metformin treatment. The hypoglycemic effect was most evident with the 300 mg LP extract/kg BW treatment.

DM causes dehydration (19) and reduced weight gain due to impaired carbohydrate metabolism (10). Treatment with LP leaf extract lessened these alterations in the rats (Table I). The outcome suggests that the extract improved diabetic rats' ability to use carbohydrates. By week 11, the diabetic rats' FBG concentration had dropped to levels comparable to those of untreated normal rats, thanks to the 300 mg/kg BW LP extract (Table I). It has been proposed that the extract's hypoglycemic effect may be due to an insulin-sensitizing or insulin-mimetic action, or to improved islet of Langerhans function recovery in diabetic rats.

Table I

Safety and efficacy of LP on organs/serum biomarkers/cytokines of STZ-induced diabetic rats

Parameters	Healthy control	Diabetic control (D)	D+200 mg metformin /kg	D+150 mg LP/kg	D+300 mg LP/kg
FBG (mmol/L)					
Week 3	7.18 ± 0.44^{a}	19.25 ± 2.56^{d}	16.68 ± 3.43^{d}	12.18 ± 2.56^{c}	8.66 ± 1.33^{b}
Week 5	6.63 ± 0.04^{a}	12.41 ± 3.80^{c}	12.26 ± 2.54^{c}	13.86 ± 3.10^{c}	9.10 ± 0.87^{b}
Week 11	5.43 ± 0.24^{a}	13.08 ± 3.00^{c}	12.56 ± 4.24^{c}	9.65 ± 2.57^{b}	5.96 ± 0.24^{a}
Week 13	5.12 ± 0.28^{a}	10.7 ± 3.11b^{c}	7.33 ± 0.85^{ab}	8.33 ± 1.54^{b}	5.51 ± 0.14^{a}
Body weights (BW)					
BW (g) week1	192.8 ± 9.9^{a}	197.8 ± 2.9^{a}	198 ± 11.2^{a}	197.8 ± 9.5^{a}	207.5 ± 4.8^{a}
BW (g) Week 13	287.6 ± 14.2^{a}	233.8 ± 9.7^{b}	239.8 ± 10.0^{b}	233.8 ± 8.9^{b}	284.5 ± 11.0^{a}
Organ somatic index (organ weight/body weight %)					
Liver	3.16 ± 0.13^{a}	5.77 ± 0.48^{b}	4.41 ± 0.11^{b}	4.35 ± 0.08^{b}	2.97 ± 0.07^{a}
Kidney	0.73 ± 0.09^{a}	0.84 ± 0.07^{b}	0.83 ± 0.07^{b}	0.66 ± 0.01^{a}	0.68 ± 0.02^{a}
Heart	0.38 ± 0.04^{a}	0.61 ± 0.09^{b}	0.48 ± 0.10^{a}	0.33 ± 0.04^{a}	0.39 ± 0.10^{a}
Spleen	0.21 ± 0.03^{a}	0.26 ± 0.04^{a}	0.27 ± 0.01^{a}	0.24 ± 0.01^{a}	0.19 ± 0.01^{a}
Lung	0.41 ± 0.04^{a}	0.66 ± 0.07^{b}	0.63 ± 0.13^{b}	0.47 ± 0.03^{a}	0.46 ± 0.05^{a}
Serum biomarkers/cytokines					
GSH (µg/mL)	79.00 ± 2.20^{a}	54.59 ± 3.59^{c}	56.29 ± 2.52^{c}	61.25 ± 2.53^{b}	70.14 ± 2.32a
MDA (ng/mL)	161 ± 44^{a}	296 ± 15^{c}	141 ± 9^{b}	129 ± 7^{a}	187 ± 70^{a}
MMP-13 (ng/mL)	5.83 ± 1.25^{a}	22.76 ± 0.90^{c}	20.75 ± 1.78^{c}	10.10 ± 4.08^{b}	14.69 ± 2.50^{b}
Claudin-1 (pg/mL)	33.12 ± 3.79^{a}	25.14 ± 0.45^{c}	27.59 ± 0.58^{b}	28.80 ± 0.60^{ab}	31.02 ± 2.66^{a}
VEGF (pg/mL)	136 ± 12^{a}	1036 ± 354^{c}	439 ± 17^{b}	427 ± 116^{b}	534 ± 49^{b}
TNF-alpha (pg/mL)	1506 ± 218^{a}	4411 ± 326^{c}	2887 ± 908^{a}	1587 ± 464^{a}	1323 ± 136^{a}
Prostaglandin-E2 (pg/mL)	44 ± 38^{a}	503 ± 17^{c}	322 ± 138^{c}	198 ± 47^{b}	87 ± 79^{b}
ALT (U/L)	38.5 ± 3.9^{a}	121.3 ± 33.4^{b}	82.0 ± 20.6^{b}	54.7 ± 12.2^{ab}	42.3 ± 4.0^{a}
AST (U/L)	101.3 ± 15.7^{a}	198.3 ± 77.4^{b}	301.0 ± 8.0^{c}	184.0 ± 12.1^{b}	104.7 ± 6.4^{a}
Creatinine (µmol/L)	52.5 ± 1.3^{a}	56.0 ± 3.3^{b}	52.8 ± 0.8^{a}	46.3 ± 9.3^{ab}	54.0 ± 1.9^{ab}
BUN (mmol/L)	7.10 ± 1.10^{a}	10.52 ± 0.71^{c}	8.83 ± 0.40^{b}	8.70 ± 1.06^{b}	7.08 ± 0.49^{a}
Albumin (g/L)	37.30 ± 0.93^{a}	31.60 ± 3.72^{b}	31.10 ± 0.80^{b}	31.10 ± 1.29^{b}	35.20 ± 2.06^{a}

Values are mean ± SEM (n = 6). Values with similar superscript letters/symbols are insignificantly different ($p < 0.05$) within the row

Over the past few decades, treatment methods for DM have made substantial progress. Conversely, taking anti-diabetic medications can lead to serious complications, including hypoglycemic coma and issues with the liver and kidneys. Medications and supplements that contain medicinal plants, vitamins, and essential elements with anti-hypoglycemic properties are vital for controlling diabetes. Plants with medicinal properties, vitamins, and essential elements that reduce blood sugar levels significantly are essential for the effective management of diabetes (20). Studies of medicinal plants, vitamins, and essential nutrients have demonstrated their effectiveness in reducing blood sugar levels in both pre-clinical and clinical trials. Research indicates that garlic has a protective impact on diabetic retinopathy in adult albino rats. Phytochemicals with anti-diabetic properties found in medicinal plants have been categorised into several main groups based on variations in their chemical composition (21). The main types of phytochemicals include alkaloids, aromatic acids, carotenoids, coumarins, flavonoids, glycosides, organic acids, phenols and phenolics, phytosterols, protease inhibitors, saponins, steroids, tannins, terpenes, and terpenoids (22). Recent research has shown that vitamins and medicinal plants possess antidiabetic properties, including antihyperglycemic, antilipidemic, hypoglycemic, and insulin-mimicking effects. The plant's LP leaves are rich in flavonoids such as myricetin, kaempferol, and quercetin, prompting further research into how this plant part affects diabetes. The administration of LP led to increases in body weight, food intake, and FBG, restoring normal serum insulin levels and worsening insulin resistance. These findings align with our earlier research. Along with enhancements in glucose metabolism, LP has also been associated with the improvement of various diabetes-related complications.

Organ Somatic Index

Disease and pathological changes in internal organs can be determined by changes in OSI (11). In STZ-induced diabetes in rats, the OSI for the liver, spleen, heart, kidneys, and lungs increased by 82.6, 23.8, 60.5, 15, and 60.97%, respectively, compared with healthy control animals, indicating that these organs were damaged. The OSI values of the internal organs of diabetic rats treated with LP extract and metformin approached those of healthy controls (Table I).

Serum inflammatory biomarker

The diabetic control group showed severe biochemical alterations compared with healthy rats. Antioxidant levels dropped markedly, with GSH decreasing to 54.59 ± 3.59 µg/mL compared with 79.00 ± 2.20 µg/mL in healthy controls, while lipid peroxidation increased sharply, as indicated by elevated MDA levels (296 ± 15 ng/mL *vs*. 161 ± 44 ng/mL). Claudin-1 levels were also significantly reduced (25.14 ± 0.45 pg/mL *vs*. 33.12 ± 3.79 pg/mL), indicating impaired epithelial barrier integrity. Diabetic rats exhibited pronounced inflammation and tissue degradation, with MMP-13 increasing to 22.76 ± 0.90 ng/mL (*vs*. 5.83 ± 1.25 ng/mL), VEGF rising to 1036 ± 354 pg/mL (*vs*. 136 ± 12 pg/mL), TNF-α elevating to 4411 ± 326 pg/mL (*vs*. 1506 ± 218 pg/mL), and PGE_2 increasing to 503 ± 17 pg/mL (*vs*. 44 ± 38 pg/mL). Metformin treatment (200 mg/kg) partially improved these abnormalities, increasing GSH to 56.29 ± 2.52 µg/mL, reducing MDA to 141 ± 9 ng/mL, and lowering inflammatory markers (MMP-13: 20.75 ± 1.78 ng/mL, VEGF: 439 ± 17 pg/mL, TNF-α: 887 ± 908 pg/mL, PGE_2: 322 ± 138 pg/mL). In contrast, LP extract showed different strengths across doses rather than a dose-dependent pattern. The 150 mg/kg dose showed the best antioxidant effect, reducing MDA to 129 ± 7 ng/mL, which is better than both metformin and the higher 300 mg/kg dose (187 ± 70 ng/mL). It also improved GSH to 61.25 ± 2.53 µg/mL and significantly lowered MMP-13 (10.10 ± 4.08 ng/mL), VEGF (427 ± 116 pg/mL), TNF-α (1587 ± 464 pg/mL), and PGE_2 (198 ± 47 pg/mL), while increasing Claudin-1 to 28.80 ± 0.60 pg/mL. The 300 mg/kg dose further improved GSH (70.14 ± 2.32 µg/mL) and showed stronger effects on some inflammatory markers (TNF-α: 1323 ± 136 pg/mL, PGE_2: 87 ± 79 pg/mL) and Claudin-1 (31.02 ± 2.66 pg/mL), although its MDA reduction was weaker than the 150 mg/kg dose. Overall, the data indicate that 150 mg/kg LP extract is superior for reducing oxidative stress (MDA), while 300 mg/kg shows greater anti-inflammatory and barrier-repair effects, demonstrating complementary but not dose-dependent responses.

The antioxidant enzyme glutathione (GSH) levels were shown to drop in diabetic rats, despite a marked increase in serum MDA levels, a marker of lipid peroxidation. An imbalance between the oxidative and antioxidative systems of cells and tissues is caused by the formation of oxidative free radicals and associated reactive oxygen species (ROS) (23). VEGF is a crucial regulator of microvasculature, promoting the survival and healing of endothelial cells (24). Meanwhile, the proteins of the MMP family primarily degrade extracellular matrix to maintain, structure, and repair tissues and organs. In addition to the impact of STZ on oxidative stress, inflammation, and apoptosis in diabetic rats used in experiments, this study also examines how an LP extract helps restore pancreatic beta cells and prevents diseases of the liver, kidneys, heart, lungs, and spleen. Through increased serum levels of the proinflammatory mediator TNF-α, lipid peroxidation and ROS generation, and decreased

antioxidant enzyme activity, hyperglycemia harms internal organs, including the pancreas, liver, kidneys, heart, lung, and spleen (23). By increasing TNF-α and its receptor, TNF-R1, hyperglycemia promotes organ and tissue pathology by activating NF-κB, which induces inflammation and cell death, ultimately damaging endothelial cells (25). STZ causes pancreatitis and the death of pancreatic acinar and islet cells by inducing the release of the proinflammatory cytokines TNF-α, IL-1, and IL-6 (26) and by reducing insulin production, leading to hyperglycemia. PGE2 is another inflammatory mediator that may affect the integrity of internal organs by acting through cell PGE2 receptors (27). Hyperglycemia increases mitochondrial ROS production. Nevertheless, mitochondrial DNA (mtDNA) is vulnerable to ROS damage, resulting in decreased mitochondrial membrane potential (ΔΨm), indicating the onset of early apoptosis. VEGF is generated by various cell types in the body, while MMP-13 is widely expressed in internal organs (28). One of the functions of MMP-13 is to assist in wound healing by coordinating cell growth and the maturation of granulation tissues. DM is associated with multiorgan injuries and damage that could stimulate the production of MMP-13 as a reparative response to tissue injuries. In the kidneys, elevated MMP-13 expression is the hallmark of diabetic nephropathy (29). The increase in VEGF and MMP-13 expressions was evident in non-treated diabetic rats in our study (Table I). LP extract reduced MMP-13 and VEGF expression in these rats, suggesting that the extract minimized organ and tissue injuries caused by diabetes mellitus. DM may abolish barrier properties of tight junction (TJ) existing between the cells by decreasing tetraspan transmembrane claudin protein in endothelial or epithelial cells. Abnormal TJ results from ROS-induced phosphorylation of tight junctions and VEGF-induced decreases in claudin-1 expression. LP extract increased serum claudin-1 concentrations, suggesting that it can protect predominantly the TJ and cell integrity (30).

Pancreas

Histologically, the pancreas of healthy rats showed islets of Langerhans that were weakly stained and surrounded by acinar structures composed of pyramidal cells with apical acidophilic cytoplasm and basal nuclei (Figure 2). In rats with STZ-induced diabetes, there was significant vacuolization of islet of Langerhans cells, necrosis of acinar cells, damage to β cells, edema, hemorrhage, enlarged interlobular and interglandular spaces, reduced cell count, and increased cell death (Table II).

Table II

Pancreas and Liver Histology Scoring of STZ-Induced Diabetic Rats Treated with LP.

Group	Pancreas (Islets)	Liver (Degeneration)	Liver (Vascular/Inf.)	Total Score (Max 12)
Healthy Control	0	0	0	0
Diabetic control (D)	3	3	2	8
D + 200 mg metformin/kg	1	1	1	3
D + 150 mg LP/kg	1	0	1	2
D + 300 mg LP/kg	1	1	1	3

GSH scavenging partially regulates cellular MDA content and raises MDA levels in STZ-induced diabetic rats, thereby indicating lipid peroxidation (31). GSH and MDA levels exhibit a significant inverse relationship associated with hyperglycemia, elevated ROS production, and reduced antioxidant levels induced by STZ (Table I). In diabetic rats, ROS induced MDA accumulation, nuclear fragmentation, and increased pancreatic cell apoptosis (32). TNF-α, a proinflammatory adipocytokine involved in insulin resistance, is generated by oxidative stress within adipose tissue. Levels of MDA and TNF-α will be elevated in diabetes (33). Treatment with a therapy rich in quercetin resulted in a significant drop in MDA levels that had become elevated, by inhibiting the release of pro-inflammatory mediators (PGE2), pro-inflammatory cytokines (TNF-α), and the NF-kB pathway, thus demonstrating an anti-inflammatory effect that could potentially aid in returning islet size and shape to normal (Table I; Figure 2) (34, 35). The extract had a greater impact than metformin in preventing STZ-induced pancreatic damage, particularly in maintaining a distinct separation between exocrine and endocrine tissues. The treatment with LP extract was demonstrated to restore normal insulin-related metabolism and islet size and shape (Figure 2) (36).

Liver (biochemical parameter and histology)

ALT and AST liver enzymes increased in untreated STZ-induced diabetic rats. In the vicinity of the portal triads, untreated STZ-induced diabetic rats showed inflammation, necrosis, pigment deposition, enlarged hepatocytes, and central vein dilatation (Figure 2). STZ causes severe pathological lesions in the liver (13). Administering LP extract at 300 mg/kg body weight reduced serum AST levels by 47.5% and ALT levels by 65.3% compared with untreated diabetic rats, suggesting that the extract has a protective effect on the liver. Significant improvements were observed: metformin increased serum AST levels substantially ($p < 0.05$), but not ALT, as indicated in Table I; these alterations were

potentially unrelated to liver damage. Metformin resulted in a moderate decrease in liver cell death but did not affect liver cell pigment buildup, severe liver cell death, or bleeding in liver tissue (Table II). In STZ-treated diabetic rats, liver sections showed damage to the central vein and adjacent portal triads (Figure 2). The modifications were not visible in the livers of rats receiving LP extract treatment (Figure 2), a finding corroborated by the decrease in liver OSI noted in Table I.

We assessed the effectiveness of LP in lowering biochemical indicators such as liver function parameters (AST, ALT) (Table I) (36).

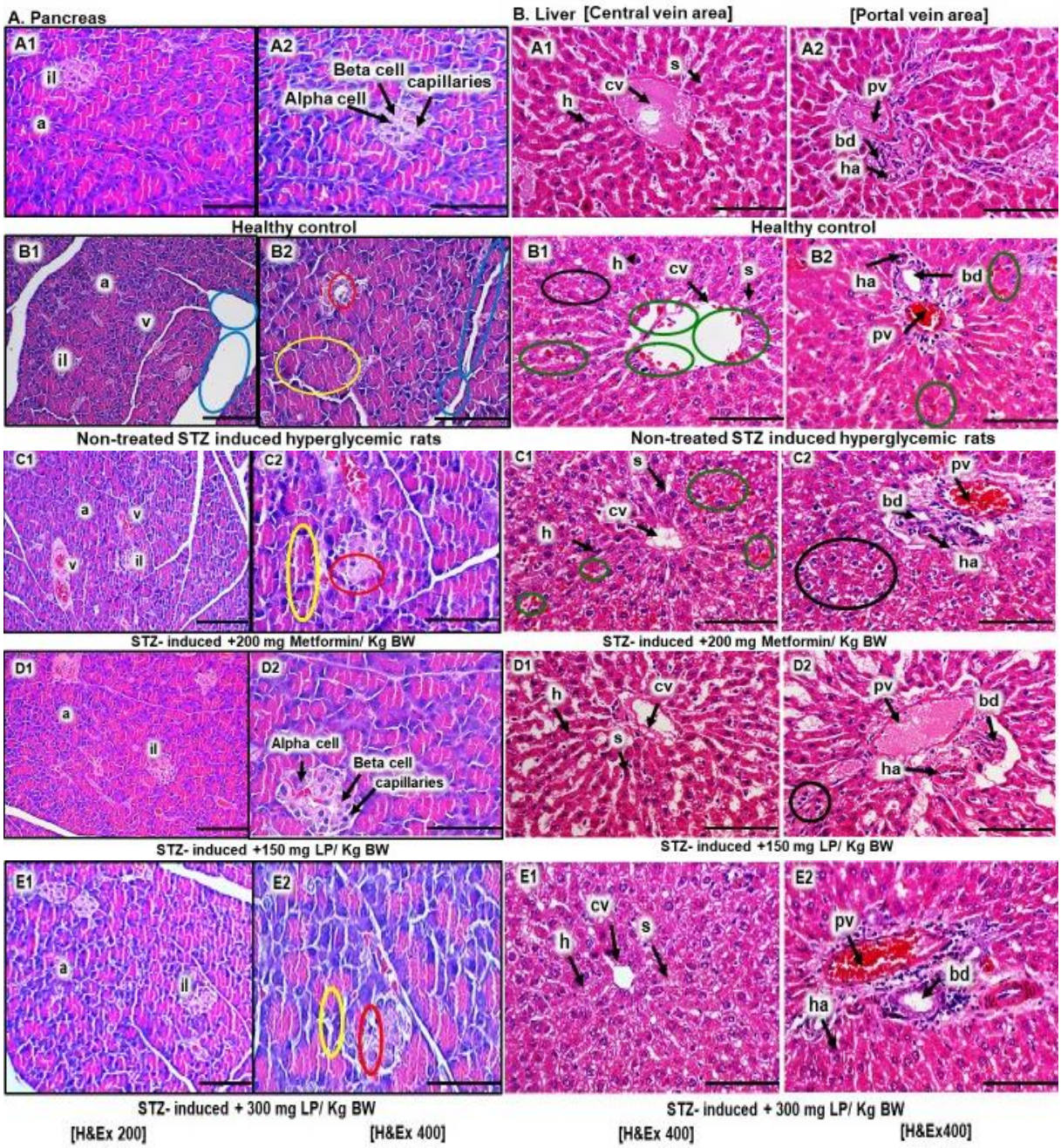

Figure 2.

Pancreas and liver tissues of STZ-diabetic rats after 10th week of treatment. (A) Pancreas: a=acinar cell, v= Blood vessel, il= Islet of Langerhans. [Oedema in interlobular and intergladular spaces of pancreatic parenchyma (blue circle); acinar necrosis (yellow circle); Islets of Langerhans necrosis (red circle)]. (B) Liver: pv= portal vein, bd=bile duct, ha= hepatic artery, cv= central vein, s= sinusoids, h=hepatocyte. Normal liver shows an intact hepatocyte. Liver injuries are indicated by [pigment deposition in hepatocyte (green circle); hepatocyte necrosis (black circle)]

According to (30), the oral administration of GSH lowered total bilirubin, ALT, AST, and serum proinflammatory cytokines, as well as serum 3-NT levels, a marker of protein damage, and enhanced vascular hypo-responsivity in an experimental obstructive jaundice animal model. Increased serum AST and ALT levels in diabetic rats may be due to increased demand for gluconeogenic substrates and to their release from damaged liver cells (36). Our findings demonstrated that oral administration of LP extract, at a dose of 300 mg/kg BW, increased serum ALT and AST levels and helped bring serum GSH levels for these parameters closer to those of healthy control rats. It has been proposed that the extract's hepatoprotective properties on the liver result from an elevation in serum GSH and a reduction in ALT, AST, and proinflammatory cytokines.

Kidneys (biochemical parameter and histology)

Serum creatinine and BUN concentrations are markers of renal function that reflect GFR; elevated levels of these parameters, especially with low serum albumin, are indicators of nephropathy (13). These changes were evident in the diabetic rats in our study (Table I). The treatment using LP extract appeared to substantially lower BUN levels without affecting creatinine levels in STZ-induced diabetic rats (Table I). The kidneys of untreated diabetic rats showed structural damage and glomerular disruption, along with severe bleeding, vacuole formation, and glycogen accumulation in the proximal and distal tubules (Table III). There is tubular epithelial glycogen deposition, interstitial nodular sclerosis, fibroplasia, hemorrhage, and collecting tubule hemorrhage and necrosis in the medulla (Table IV). LP extract and metformin treatment reduced the development of these lesions in the renal cortex and medulla (Figures 3 and 4).

Excess ROS and oxidative stress in the kidney, caused by high blood glucose levels, lead to apoptosis and bleeding of the epithelial and mesangial cells in the proximal tubule, hastening the onset of diabetic nephropathy (37). Proinflammatory cytokines trigger renal inflammation when diabetic nephropathy develops. In patients with diabetic nephropathy, elevated levels of TNF-α, PGE2, and VEGF have been observed in the serum and renal cortex (38). According to earlier research, pro-inflammatory cytokines (TNF-α and IL-1β) influence changes in renal function and are regulated by MMPs (39). The glomerulus's MMPs function as the main controllers of its ECM (extracellular matrix) formation and deterioration. Modifications in MMP expression or MMP activity also regulate the composition of the intrarenal ECM (40). MMPs play a critical role in kidney remodeling, specifically impacting the kidney's glomerular, tubulointerstitial, and vascular regions by altering ECM (extracellular matrix) degradation (41). ECM alteration causes the accumulation of collagen types I and III, along with a higher collagen-to-elastin ratio, which increases volume flow resistance. Collagen I, collagen II, entactin, aggrecan, tenascin, pro-TNF-α, pro-MMP-9, and pro-MMP-13 are the substrates selected for collagenase MMP. Furthermore, MMPs and TIMPs affect a wide range of functions, including chemokine and cytokine production and release, chemotaxis, apoptotic signaling, and the activity and proliferation of various cell lines (42). MMP inhibitors with a particular affinity for MMP-9 and/or MMP-13 could potentially provide more effective treatment options in preventing the progression of glomerulosclerosis (43). MMP-13, released by damaged podocytes, may impair glomerular basement membrane components such as basement membrane proteoglycans or catalyze the activation of other proteases or growth factors that contribute to glomerular damage (44). Increased BUN, albumin excretion, and serum creatinine all indicate kidney impairment in STZ-induced diabetes. Research indicates that in diabetic rats, LP protects the kidneys and renal function markers (albumin, creatinine, and BUN). Improvements in renal function and kidney histology suggest that the ethanol extract of LP has renoprotective effects against STZ-induced renal injury. The ethanol extract of LP demonstrates a renoprotective effect against STZ-induced renal injury, as evidenced by improvements in renal function (Table I) and kidney histology. Significant hemorrhage, necrosis, vacuolization, and glycogen accumulation were observed in the proximal convoluted tubule, vasa recta, collecting duct, ascending thick segment of the loop of Henle, glomerular capsular space, parietal layer of the glomerular capsule, and ascending thin segment of the loop of Henle, according to the Histopathological examination of the kidneys from diabetic rats (Figure 2); (Figure 3). Additionally, LP significantly improved the medulla, tubular cells, and glomerular gaps, and altered glomeruli in diabetic rats (Figure 3). According to our deduced results, LP leaves protect STZ-induced diabetic rats from diabetic nephropathy by lowering inflammation (as measured by serum TNF-α, PGE2, VEGF, and MMP-13 levels) and oxidative stress and lipid peroxidation through increased antioxidant enzyme activity. Additionally, LP restored the integrity of certain structures and the growth of nephritis. These findings are consistent with the results of previously published studies (45).

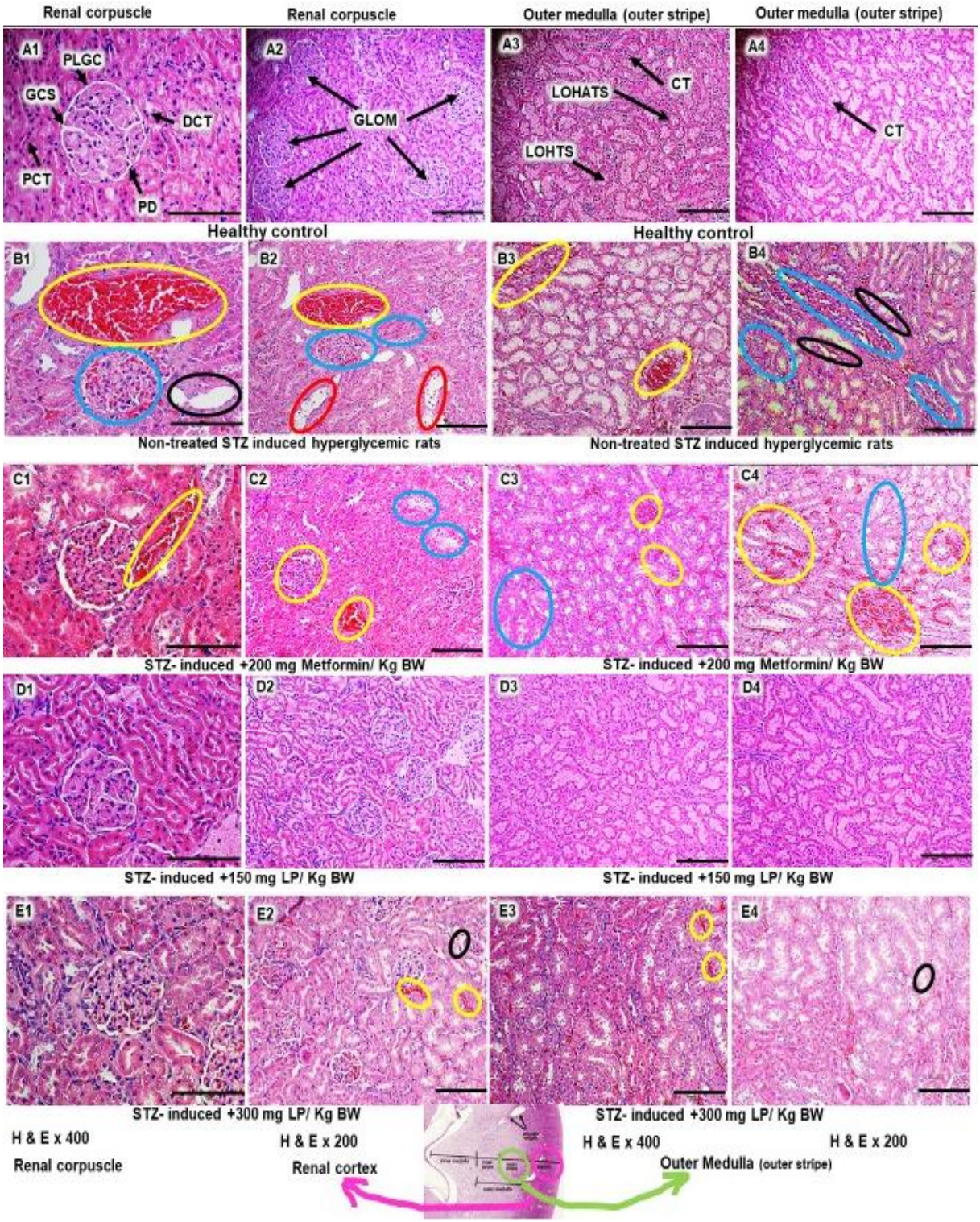

Figure 3.

Safety and efficacy of LP on renal cortex and medulla of STZ-induced diabetic rats. PLGC=parietal layer of glomerular capsule, GCS= glomerular capsular space, PCT= proximal convoluted tubule, DCT= distal convoluted tubule, PD= podocyte, GLOM= glomerulus, CT=collecting tubule, VR= Vasa Recta, LOHATS= loop of Henle ascending thick segment, LOHTS= loop of Henle thin segment. A normal kidney shows unremarkable renal corpuscles, renal cortex, renal medulla, and renal tubules. Kidney cell changes include the presence of [hemorrhage (yellow circle) and necrosis (blue circle) of cortex and outer medulla, glycogen deposition (red circle) in cortex, vacuolization (black circle) of tubule]

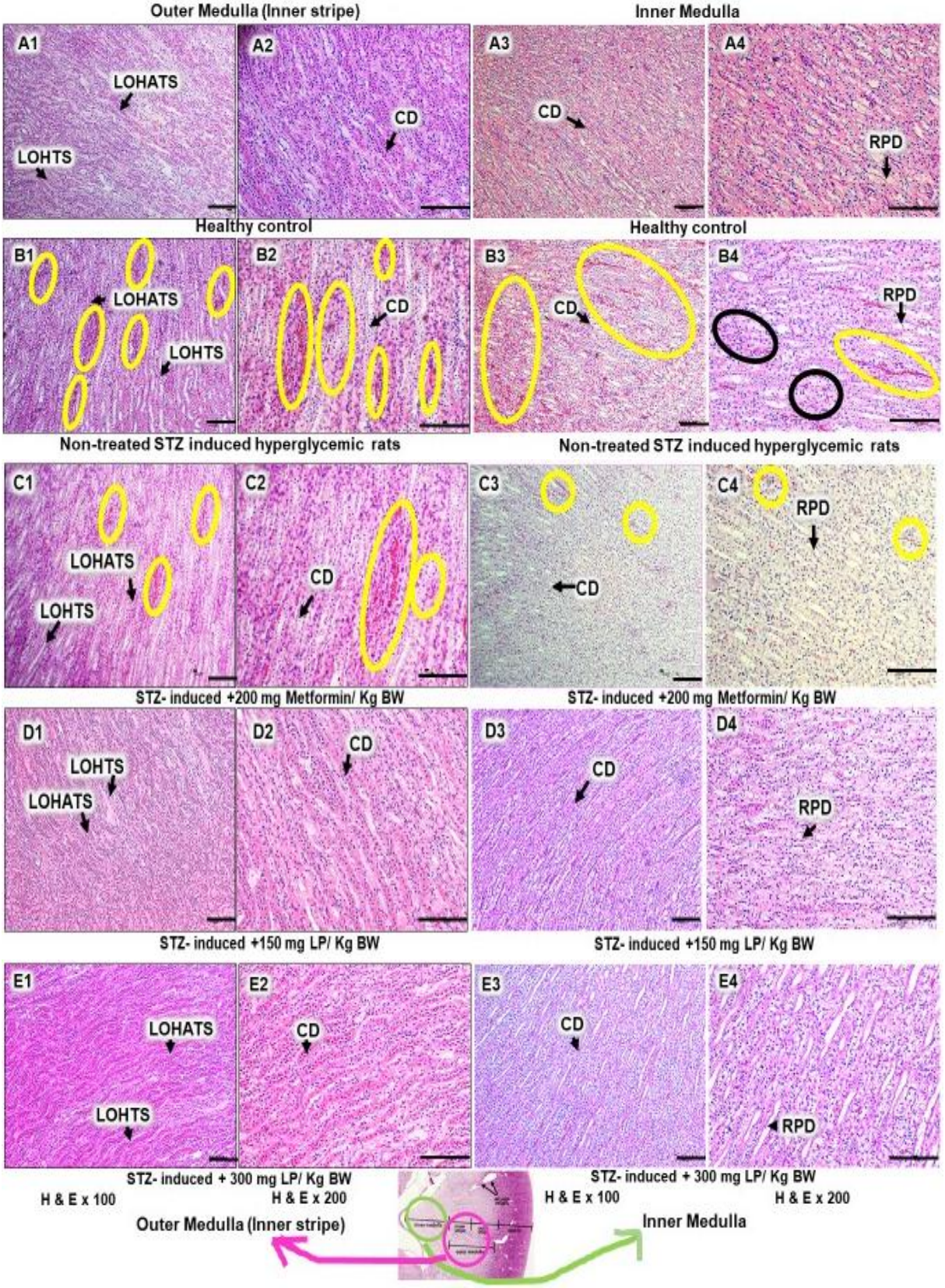

Figure 4.

Safety and efficacy of LP on the loop of Henle, collecting duct, and renal papillary duct of STZ-diabetic rats. LOHATS = loop of Henle ascending thick segment, LOHTS = loop of Henle thin segment, CD= Collecting duct, RPD= Renal papillary duct. A normal kidney shows unremarkable LOHATS, LOHTS, CD, and RPD. Renal tubule changes include the presence of hemorrhage (yellow circle) and vacuolization (black circle).

Table III

Renal Histology Scoring of STZ-Induced Diabetic Rats Treated with LP

Group	Glomerular Damage (GLOM)	Tubular Necrosis (PCT/DCT/CT)	Tubular Vacuolization	Interstitial Edema/Hemorrhage	Glycogen Deposition	Total Score (Max 15)
Healthy Control	0	0	0	0	0	0
Diabetic control (D)	3	3	2	3	2	13
D + 200 mg metformin/kg	2	2	1	2	1	8
D + 150 mg LP/kg	1	1	1	1	1	5
D + 300 mg LP/kg	0	0	0	0	0	0

Table IV

Medullary Histology Scoring of STZ-Induced Diabetic Rats

Group	Tubular Necrosis (LOH, CD, RPD)	Tubular Vacuolization	Tubular Dilation / Lumen Widening	Interstitial Edema / Hemorrhage	Total Score (Max 12)
Healthy Control	0	0	0	0	0
Diabetic control (D)	3	2	3	2	10
D + 200 mg metformin/kg	2	1	2	1	6
D + 150 mg LP/kg	1	1	1	1	4
D + 300 mg LP/kg	0	0	0	0	0

Heart

A complication of DM is cardiovascular disease (CVD). We observed clear myofibril disorganization, myocyte hypertrophy, angiogenesis, and hemorrhage in the epicardium and myocardium of non-treated STZ-induced diabetic rats, all of which were reflected by the increase in OSI. The increased heart weight (Figure 5) also suggests myocardial hypertrophy (19). LP extract treatment markedly attenuated these lesions in the rats (Figure 4). However, in metformin-treated diabetic rats, the myocardium still showed vacuolization and hemorrhage, suggesting it is less effective than the LP extract in the protection of the heart against diabetic injuries (Table V).

A systemic inflammatory condition, such as diabetic cardiomyopathy (DCM), is a significant and severe complication of diabetes that impacts the heart, leading to heightened morbidity and mortality. Cardiac fibrosis is mediated by the interactions between several cytokines, including TNF-α, IL-6, IL-8, IL-1β, and chemokine C-reactive protein (CRP) (46, 47, 48). Additionally, PGE2 activates EP3, and overexpression of EP3 in cardiomyocytes causes a marked decrease in the ejection fraction and an increase in the end-diastolic and end-systolic ventricular volume following ischemic injury. On the other hand, activating EP3 or EP4 in cultured isolated mice cardiomyocytes improves contractile properties and Ca^{2+} handling, but overexpressing EP4 increases fractional shortening, ejection fraction, and left ventricular internal diameter during systole (49).

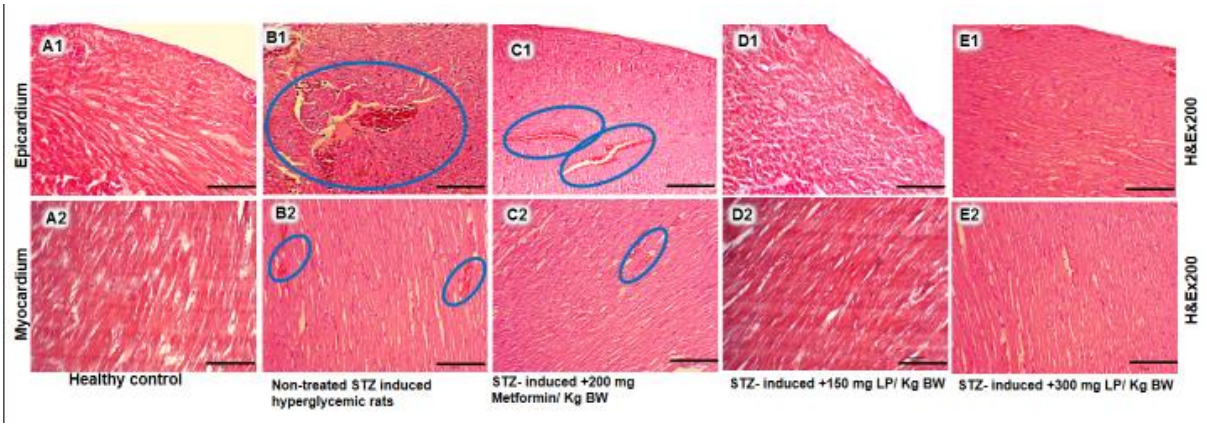

Figure 5.

Safety and efficacy of LP on heart tissues of STZ-induced diabetic rats. A healthy rat shows unremarkable cardiomyocytes. Cardiomyocyte changes include the presence of hemorrhage in the epicardium and myocardium (blue circle).

Table V

Heart Tissue Histology Scoring of STZ-Induced Diabetic Rats.

Group	Epicardial Damage	Myocardial Degeneration	Inflammation	Vascular Changes	Total Score (Max 12)
Healthy Control	0	0	0	0	0
Diabetic control (D)	3	3	3	3	12
D + 200 mg metformin/kg	2	1	2	1	6
D + 150 mg LP/kg	1	1	1	1	4
D + 300 mg LP/kg	1	0	0	0	1

Furthermore, observed that in 8-week-old db/db mice, cardiac function was impaired and that a 2-week *in vivo* treatment with an EP3 antagonist led to modest improvements (50). Increased levels of ECM components, including collagen I and III, and pro-fibrotic proteins such as TGF-β contribute to pathological fibrosis in the context of DCM. Increased levels of pro-fibrotic factors such as TGF-β and ECM components such as collagen I and III contribute to pathological fibrosis in association with DCM (43). LP extract reduced systemic inflammatory biomarkers (TNF-α and PGE2) in the detection of cardiovascular disease, as summarized in Table I. DCM results from interstitial alterations, including dilated cardio-myopathy and cardiac fibrosis, localized fat infiltration, and, infrequently, localized inflammatory infiltration. The most common alteration in dilated cardiomyopathy is the development of fibrosis, which varies in degree, occurring both interstitially and around blood vessels. Fibrosis is an essential component of myocardial remodeling in dilated cardiomyopathy, as it is in other heart diseases, but it also has distinct characteristics (51). The composition and characteristics of the extracellular matrix influence the mechanical properties of the myocardium during both diastole and systole. Changes that lead to myocardial fibrosis can cause heart failure by reducing oxygen delivery to cardiomyocytes and disrupting their electrical connections. (Figure 5). Thus, we may speculate that the anti-fibrotic effects of LP are also related to its inhibitory effect on NF-κB, TGF-β activation pathway (Figure 5); (Table I) (52).

Lungs

The lungs of untreated diabetic rats showed damage to cellular structure, with focal hemorrhages in the bronchiolar lumen, terminal bronchiole, alveolar duct, and alveoli sections, bronchiole stenosis, severe fibrosis, alveolar thickening, pneumocyte 1 and pneumocyte 2 damage, and septal necrosis. The metformin-treated diabetic rats had severe thickening of the alveolar wall and alveolar sac and septum necrosis, but without hemorrhage. Diabetic rats treated with LP extract showed significantly reduced lung injuries (Figure 6); (Table VI). Pulmonary endothelial cells (ECs) in the pulmonary microvasculature exhibit lower permeability and distinct responses to barrier-disruptive stimuli compared with those in other organs (53, 54). Diabetic rats exhibited lungs with an expanded interstitium, larger alveolar gaps, mononuclear cell infiltration, increased cell proliferation, hypertrophy of interstitial cells, and accelerated fibrosis due to heightened pulmonary vascular permeability.

Diabetes has also been linked to variations in the thickness of the alveolar-capillary basement membrane and nodular fibrosis in the alveolar walls, according to findings from human autopsies and transbronchial biopsies. The endothelial dysfunction-driven hyperglycemia can cause oxidative stress and lung lesions (55). These were evident as hemorrhage [bronchiole, terminal bronchiole, alveoli, pneumocyte], thickening of the wall of bronchiole and interalveolar septa, stenosis of bronchiole and wall, cellular infiltration in the septa, increased collagen fibers, reduced pulmonary elastic recoil, and emphysematous alveoli. Clinically, these alterations could result in decreased diffusion and spirometry scores (56). Some processes are triggered by hyperglycemic pseudohypoxia (HPSD), including elevated TGF-β and VEGF production, protein kinase C activation, oxidative stress, activation of the coagulation cascade, TNF-α expression, and elevated insulin levels. HPSD causes reduced lung volume, impaired pulmonary diffusion, and reduced pulmonary elastic recoil due to decreased capillary blood volume. Angiogenic growth factors, such as VEGF, regulate endothelial dysfunction, which can lead to insulin resistance, platelet hyperactivity, oxidative stress, excessive generation of free fatty acids, vaso-constriction, and pulmonary thrombosis (56, 57). Hyperglycemia and the non-enzymatic glycosylation of the connective tissue matrix (collagen and elastin) lead to micro-vascular sequelae, or microangiopathy. Reduced pulmonary capillary blood flow, chronic low-grade inflammation, autonomic neuropathy, and reduced lung elasticity are all consequences of micro-angiopathy, which causes the alveolar epithelium and basal lamina to thicken. During breathing, these changes impair the lung's flexibility and gas exchange (58). Histological samples from untreated STZ-induced hyperglycemic rats show pulmonary microangiopathy, bronchiole smooth muscle thickening, pulmonary capillary bleeding, and changes in pulmonary connective tissue caused by

glycosylation. (Figure 6). With doses of 150 mg and 300 mg, we believe that LP can treat microvascular sequelae, microangiopathy, and hyperglycemic pseudo-hypoxia (HPSD) by blocking the underlying mechanism.

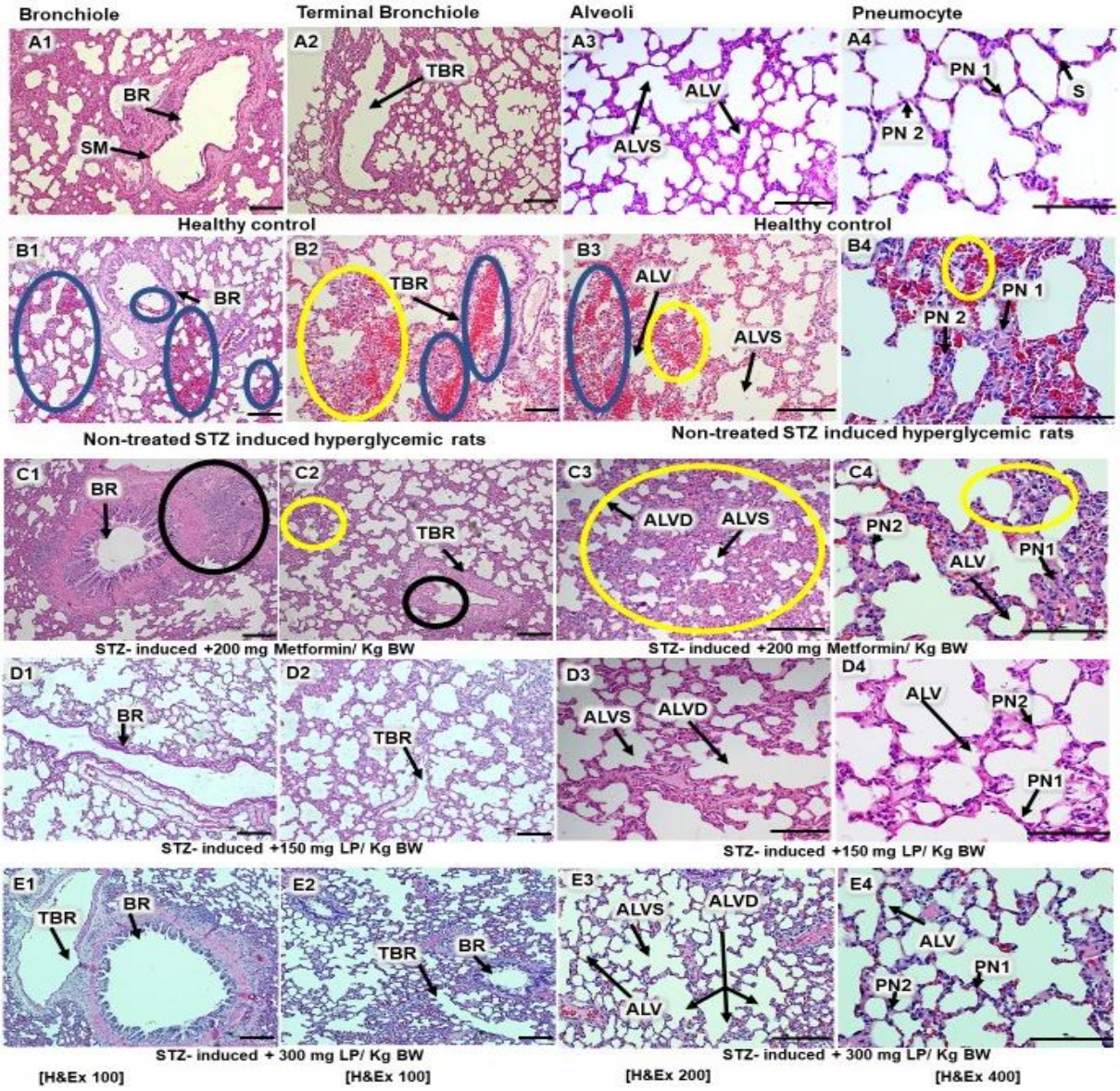

Figure 6.

Safety and efficacy of LP on lung tissues of STZ-induced diabetic rats. BR=bronchiole, TBR= terminal bronchiole, S= septum, SM= smooth muscle, ALVS= Alveolar sac, ALVD= Alveolar duct, ALV= Alveoli, PN1=Pneumocyte 1, PN2=Pneumocyte 2. Healthy control rat shows unremarkable BR, TBR, S, SM, ALVS, ALVD, ALV, PN1, PN2. Lung changes include focal hemorrhage in the TBR, BR, S, ALVS, ALVD, and ALV (blue circle), fibrosis of the alveolar wall (yellow circle), and stenosis of the bronchiole and alveoli (black circle)

Table VI

Lungs Tissue Histology Scoring of STZ-Induced Diabetic Rats

Group	Bronchiolar Damage	Alveolar Damage	Pneumocyte Alteration	Inflammation	Total Score
Healthy Control	**0**	**0**	**0**	**0**	**0**
Diabetic control (D)	**3**	**3**	**3**	**3**	**12**
D + 200 mg metformin/kg	**1**	**2**	**1**	**1**	**5**
D + 150 mg LP/kg	**1**	**1**	**1**	**1**	**4**
D + 300 mg LP/kg	**1**	**1**	**1**	**0**	**3**

Spleen

The STZ treatment severely damaged the spleen's architecture, with the development of hyperplastic changes, hydrophobic-hydrophilic degradation, hemorrhage, and necrosis (Figure 7). In addition, the red pulp zone exhibited severe hemorrhages and disorganized monocyte distribution in the splenic cords. Diabetic rats that received treatment showed hyperplasia in the white pulp and vacuolization in the red pulp, along with loss of zonal separation between the white and red pulp. Rats with diabetes who received the LP extract showed a decrease in the severity of the spleen lesions. In these rats, there was still an increase in tissue growth in the white pulp and some blood-producing cells in the red pulp, as indicated in Figure 7 and Table VII.

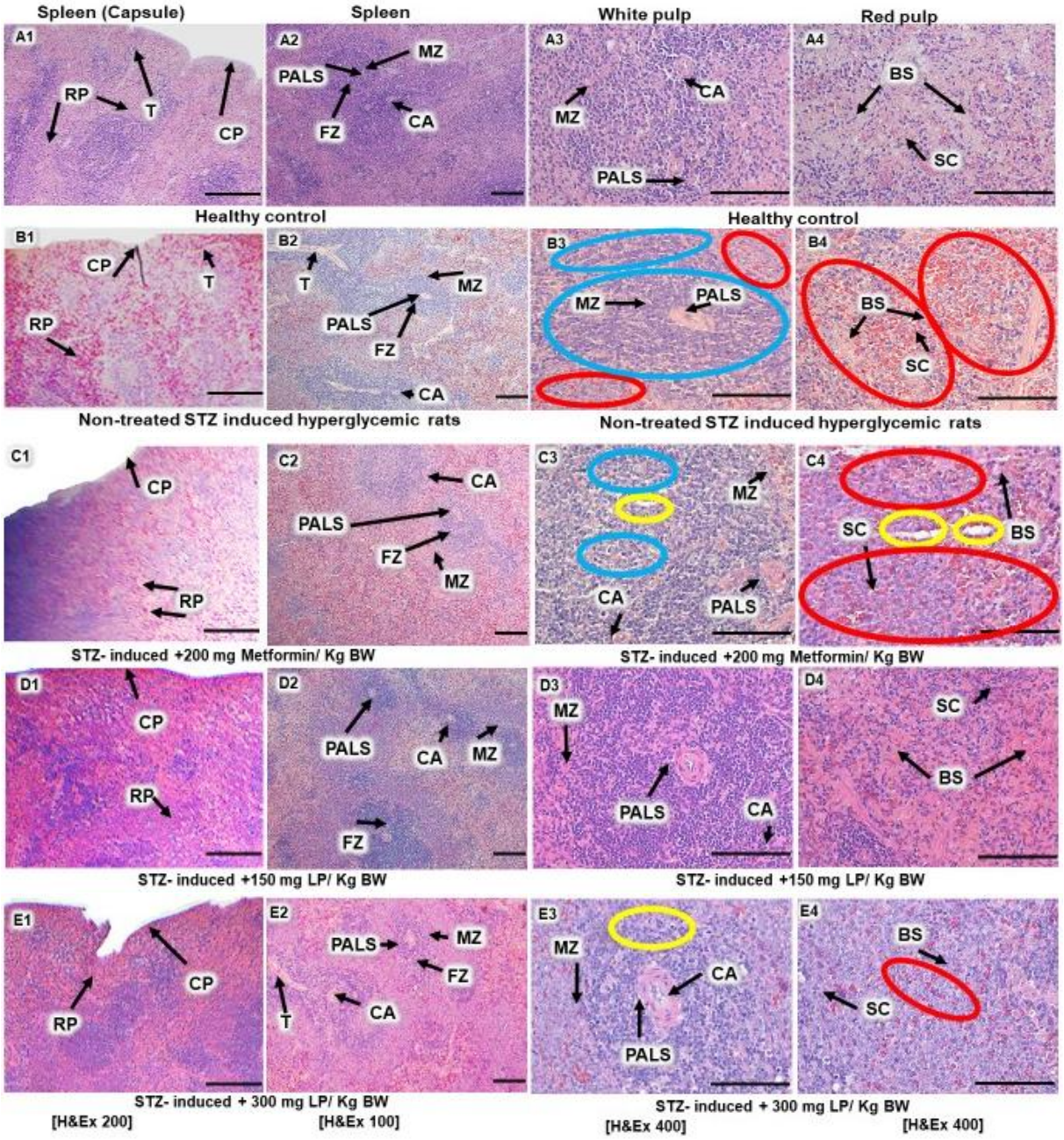

Figure 7.

Safety and efficacy of LP on spleen tissues of STZ-induced diabetic rats. SN = Splenic nodule, CA= Central artery, MZ= Splenic marginal zone, FZ=Follicular zone, RP=Red pulp, T=trabeculae, BS = Blood sinus, SC = splenic cord, PALS = the periarteriolar lymphoid sheaths. A healthy control spleen shows unremarkable white pulp and red pulp cells. Spleen injuries are indicated by necrotic cells (NC) in the white pulp region (blue circle), hydropic degeneration in the white pulp region (yellow circle), and an increase in hematopoietic cells (red circle) in the red pulp region

Table VII

Spleen Tissue Histology Scoring of STZ-Induced Diabetic Rats

Group	Capsule Damage	White Pulp Alteration	Red Pulp Damage	Inflammation	Total Score (Max 12)
Healthy Control	0	0	0	0	0
Diabetic control (D)	3	3	3	3	12
D + 200 mg metformin/kg	1	2	2	1	6
D + 150 mg LP/kg	1	1	1	1	4
D + 300 mg LP/kg	1	1	1	0	3

Spleen damage caused by diabetes results in immunodeficiency, heightening the likelihood of infection and death among diabetic patients. In a diabetic spleen, an excess of free radicals causes lipid and protein peroxidation, disrupting normal cellular function, abnormal cell signaling, and impaired biological activity. For instance, splenic damage and a decline in the antioxidant defense system are caused by ROS (59). As a result, lipid peroxidation levels (measured by MDA) are used as standard biological indicators of oxidative stress. Diabetes-related spleen damage is exacerbated by oxidative stress and by inflammatory substances generated by immune cells, including TNF-α, IL-1β, IL-6, and MCP-1. Moreover, disrupts insulin receptor signaling pathways, leading to abnormal IRS phosphorylation and impaired insulin function. Splenocytes significantly influence pancreatic β-cell regeneration in insulin-deficient rats. Pancreatectomy combined with splenectomy resulted in a higher rate of diabetes compared to those who solely had pancreatectomy, indicating that the spleen may contribute to β-cell regeneration (60). Despite existing interventions, better therapeutic strategies are needed to address unmet clinical needs (61). LP's ameliorative role in diabetes-associated splenic damage is due to restoring the balance of oxidative stress and improving the inflammatory response. LP significantly exacerbated the morphological and histopathological changes in the spleen and pancreas of diabetic rats (Figure 6); (Figure 1). While also reducing splenocyte apoptosis, thus mitigating diabetes-related splenic damage (Figure 7). Furthermore, LP reduced necrotic cells in the white pulp, sinusoidal hemorrhage, and hematopoietic cell accumulation in the red pulp. LP may reverse spleen atrophy by increasing spleen weight and extending spleen length. LP significantly lowered serum MDA levels, and [necrotic cell and hydropic degradation] in the white pulp area, along with hematopoietic cells in the red pulp area.

Conclusions

Rats with STZ-induced hyperglycemia developed oxidative stress, tissue deterioration, and inflammation, according to the study. Thus, LP extract attenuated some diabetes-associated changes in organ morphology and serum biomarkers. Because of its capacity to suppress inflammation, lipid peroxidation, and oxidative stress, the LP extract was found to have protective benefits that exceeded those of metformin in reducing internal organ damage associated with diabetes.

Limitation of the study

A limitation of the present study is the lack of quantitative phytochemical standardization of the LP extract, including the absence of mg/g estimation of gallic acid, myricetin, or total phenolic content and detailed batch-to-batch variability analysis. However, this was intentional, as the primary objective of the study was to evaluate the overall biological activities of the crude LP extract rather than to investigate the effects of individual isolated compounds. Qualitative HPLC fingerprinting was employed to ensure extract identity and compositional consistency for biological evaluation. Future studies should incorporate quantitative standardization and batch-to-batch assessment to enable dose–response correlations, improve reproducibility, and enhance the translational relevance of LP extract–based investigations.

Acknowledgement

Not applicable.

Funding

This study was supported by Princess Nourah bint Abdulrahman University Researchers Supporting Project number (PNURSP2026R30), Princess Nourah bint Abdulrahman University, Riyadh, Saudi Arabia.

Availability of data and materials

The data generated in the present study are included in the figures and/or tables of this article.

Ethics approval and consent to participate

All experimental procedures were approved by Prof. Dr. Mohd Hair Bejo, Chairman of University Putra Malaysia's Institutional Animal Care and Use Committee on 7th February 2018 under protocol Committee (approval No. UPM/IACUC/AUP-R095/2017).

AI use disclosure

During the preparation of this manuscript, the author(s) have not used any AI tools. The author(s) reviewed and revised by themselves and take(s) full responsibility for the final content of the work.

Conflict of interest

The authors declare no conflict of interest.

References

1. Saeedi P, Petersohn I, Salpea P, Malanda B, Karuranga S, Unwin N, et al. Global and regional diabetes prevalence estimates for 2019 and projections for 2030 and 2045: Results from the International Diabetes Federation Diabetes Atlas, 9th edition. Diabetes Res Clin Pract. 2019;157:107843.
2. Chaudhury A, Duvoor C, Reddy Dendi VS, Kraleti S, Chada A, Ravilla R, et al. Clinical Review of Antidiabetic Drugs: Implications for Type 2 Diabetes Mellitus Management. Front Endocrinol (Lausanne). 2017;8:6.
3. Cade WT. Diabetes-related microvascular and macrovascular diseases in the physical therapy setting. Phys Ther. 2008;88(11):1322-1335.
4. Fowler MJ. Microvascular and macrovascular complications of diabetes. Clin Diabetes. 2008;26(2):77-82.
5. Contreras-Zentella ML, Hernández-Muñoz R. Is liver enzyme release really associated with cell necrosis induced by oxidant stress?. Oxid Med Cell Longev. 2016;2016:3529149.
6. Chua LS, Latiff NA, Lee SY, Lee CT, Sarmidi MR, Aziz RA. Flavonoids and phenolic acids from Labisia pumila (Kacip Fatimah). Food Chem. 2011;127(3):1186-1192.
7. Karimi E, Jaafar HZE, Ahmad S. Phytochemical analysis and antimicrobial activities of methanolic extracts of leaf, stem and root from different varieties of Labisia pumila Benth. Molecules. 2011;16(6):4438-4450.
8. Abdel Aziz SM, Ahmed OM, Abd El-Twab SM, Al-Muzafar HM, Amin KA, Abdel-Gabbar M. Antihyperglycemic effects and mode of actions of Musa paradisiaca leaf and fruit peel hydroethanolic extracts in nicotinamide/streptozotocin-induced diabetic rats. Evid Based Complement Alternat Med. 2020;2020:9276343.
9. Qiu YY, Tang LQ, Wei W. Berberine exerts renoprotective effects by regulating the AGEs-RAGE signaling pathway in mesangial cells during diabetic nephropathy. Mol Cell Endocrinol. 2017;443:89-105.
10. Virdi J, Sivakami S, Shahani S, Suthar AC, Banavalikar MM, Biyani MK. Antihyperglycemic effects of three extracts from Momordica charantia. J Ethnopharmacol. 2003;88(1):107-111.
11. Teh BP, Ahmad N, Ibnu Rasid EN, Zolkifli NA, Sastu Zakaria UR, Yusoff NM, et al. Herbal-based formulation containing Eurycoma longifolia and Labisia pumila aqueous extracts: Safe for consumption?. Pharmaceuticals (Basel). 2021;14(2):142.
12. Gholamzadeh S, Zarenezhad M, Montazeri M, Zareikordshooli M, Sadeghi G, Malekpour A, et al. Statistical analysis of organ morphometric parameters and weights in South Iranian adult autopsies. Medicine (Baltimore). 2017;96(21):e6447.
13. Zafar M, Naeem-Ul-Hassan Naqvi S. Effects of STZ-induced diabetes on the relative weights of kidney, liver and pancreas in albino rats: A comparative study. Int J Morphol. 2010;28(1):135-142.
14. Dyson NJ, Kattner N, Honkanen-Scott M, Hunter B, Doyle JA, White K, et al. Development and application of a semi-quantitative scoring method for ultrastructural assessment of acute stress in pancreatic islets. Transplant Direct. 2021;8(1):e1271.
15. Tervaert TWC, Mooyaart AL, Amann K, Cohen AH, Cook HT, Drachenberg CB, et al. Pathologic classification of diabetic nephropathy. J Am Soc Nephrol. 2010;21(4):556-563.
16. Abdel-Daim MM, Abushouk AI, Donia T, Alarifi S, Alkahtani S, Aleya L, et al. The nephroprotective effects of allicin and ascorbic acid against cisplatin-induced toxicity in rats. Environ Sci Pollut Res Int. 2019;26(13):13502-13509.
17. Silva IAN, Gvazava N, Bölükbas DA, Stenlo M, Dong J, Hyllen S, et al. A semi-quantitative scoring system for green histopathological evaluation of large animal models of acute lung injury. Bio Protoc. 2022;12(16):e4493.
18. Al-Rikabi AC, Al-Ani WM, Al-Rawi NM. Ameliorative effect of natural compounds on lead-induced splenic toxicity in rats. Biomed Pharmacother., 2020; 568(125): 46-56
19. Mubbunu L, Bowa K, Petrenko V, Silitongo M. Correlation of internal organ weights with body weight and body height in normal adult Zambians: A case study of Ndola Teaching Hospital. Anat Res Int. 2018;2018:4687538.
20. Yedjou CG, Grigsby J, Mbemi A, Nelson D, Mildort B, Latinwo L, et al. The management of diabetes mellitus using medicinal plants and vitamins. Int J Mol Sci. 2023;24(10):9085.
21. Oladeji OS, Adelowo FE, Ayodele DT, Odelade KA. Phytochemistry and pharmacological activities of Cymbopogon citratus: A review. Sci Afr. 2019;6:e00137.
22. Kumar A, Nirmal P, Kumar M, Jose A, Tomer V, Oz E, et al. Major phytochemicals: Recent advances in health benefits and extraction methods. Molecules. 2023;28(2):887.
23. Scărlătescu AI, Voicu SN, Pițuru MT, Apetroaei MM, Velescu BS, Udeanu DI, et al. Probiotic effects on oxidative stress pathways in diabetes. Farmacia. 2024;72(6):1437-1449.
24. Duffy AM, Bouchier-Hayes DJ, Harmey JH. Vascular endothelial growth factor (VEGF) and its role in non-endothelial cells: Autocrine signalling by VEGF. In: Madame Curie Bioscience Database [Internet]. Austin (TX): Landes Bioscience; 2000-2013. Available from: https://www.ncbi.nlm.nih.gov/books/NBK6482/
25. Ghosh S, Bhattacharyya S, Rashid K, Sil PC. Curcumin protects rat liver from streptozotocin-induced diabetic pathophysiology by counteracting reactive oxygen species and inhibiting the activation of p53 and MAPKs

mediated stress response pathways. Toxicol Rep. 2015;2:365-376.
26. Wang-Fischer Y, Garyantes T. Improving the reliability and utility of streptozotocin-induced rat diabetic model. J Diabetes Res. 2018;2018:8054073.
27. Nasrallah R, Hassouneh R, Hébert RL. PGE2, kidney disease, and cardiovascular risk: Beyond hypertension and diabetes. J Am Soc Nephrol. 2016;27(3):666-676.
28. Yu T, Robotham JL, Yoon Y. Increased production of reactive oxygen species in hyperglycemic conditions requires dynamic change of mitochondrial morphology. Proc Natl Acad Sci U S A. 2006;103(8):2653-2658.
29. Garcia-Fernandez N, Jacobs-Cachá C, Mora-Gutiérrez JM, Vergara A, Orbe J, Soler MJ. Matrix metalloproteinases in diabetic kidney disease. J Clin Med. 2020;9(2):472.
30. González-Mariscal L, Betanzos A, Nava P, Jaramillo BE. Tight junction proteins. Prog Biophys Mol Biol. 2003;81(1):1-44.
31. Banerjee A, Singh S, Prasad SK, Kumar S, Banerjee O, Seal T, et al. Protective efficacy of Tinospora sinensis against streptozotocin induced pancreatic islet cell injuries of diabetic rats and its correlation to its phytochemical profiles. J Ethnopharmacol. 2020;248:112356.
32. Erejuwa OO, Sulaiman SA, Wahab MS, Sirajudeen KNS, Salleh MSMD, Gurtu S. Antioxidant protection of Malaysian tualang honey in pancreas of normal and streptozotocin-induced diabetic rats. Ann Endocrinol (Paris). 2010;71(4):291-296.
33. Armenia A, Badriyya E, Rahmita S, Rachmaini F, Abdillah R. Malondialdehyde and TNF-α lowering effects of purified gambier (Uncaria gambir Roxb.) in diabetic rats. J Ayurveda Integr Med. 2024;15(1):100855.
34. Comalada M, Camuesco D, Sierra S, Ballester I, Xaus J, Gálvez J, et al. In vivo quercitrin anti-inflammatory effect involves release of quercetin, which inhibits inflammation through down-regulation of the NF-κB pathway. Eur J Immunol. 2005;35(2):584-592.
35. Wu H, Xi H, Lai F, Ma J, Liu H. Chemical and cellular antioxidant activity of flavone extracts of Labisia pumila before and after in vitro gastrointestinal digestion. RSC Adv. 2018;8:12116-12126.
36. Jabbar AAJ, Alamri ZZ, Abdulla MA, Salehen NA, Salim Amur Al Sinawi Z, Alfaifi SM. Hepatoprotective effects of Gynura procumbens against thioacetamide-induced cirrhosis in rats: Targeting inflammatory and oxidative stress signalling pathways. Heliyon. 2023;9(9):e19418.
37. Wang N, Zhang C. Oxidative stress: A culprit in the progression of diabetic kidney disease. Antioxidants (Basel). 2024;13(4):455.
38. Donate-Correa J, Martín-Núñez E, Muros-De-Fuentes M, Mora-Fernández C, Navarro-González JF, Inflammatory cytokines in diabetic nephropathy. J Diabetes Res. 2015;2015:948417.
39. Lee HS, Kim WJ. The role of matrix metalloproteinase in inflammation with a focus on infectious diseases. Int J Mol Sci. 2022;23(18):10546.
40. Park JYC, King A, Björk V, English BW, Fedintsev A, Ewald CY. Strategic outline of interventions targeting extracellular matrix for promoting healthy longevity. Am J Physiol Cell Physiol. 2023;325(1):C90-C128.
41. Tan RJ, Liu Y. Matrix metalloproteinases in kidney homeostasis and diseases. Am J Physiol Renal Physiol. 2012;302(11):F1351-61.
42. Geraldes P, King GL. Activation of protein kinase C isoforms and its impact on diabetic complications. Circ Res. 2010;106(8):1319-1331.
43. Ayuk SM, Abrahamse H, Houreld NN. The role of matrix metalloproteinases in diabetic wound healing in relation to photobiomodulation. J Diabetes Res. 2016;2016:2897656.
44. Sakamaki Y, Sasamura H, Hayashi K, Ishiguro K, Takaishi H, Okada Y, et al. Absence of gelatinase (MMP-9) or collagenase (MMP-13) attenuates adriamycin-induced albuminuria and glomerulosclerosis. Nephron Exp Nephrol. 2010;115(2):e22–e32.
45. Alanazi AZ, Al-Rejaie SS, Ahmed MM, Alhazzani K, Alhosaini K, As Sobeai HM, et al. Protective role of Dodonaea viscosa extract against streptozotocin-induced hepatotoxicity and nephrotoxicity in rats. Saudi Pharm J. 2023;31(8):101669.
46. Ramesh P, Yeo JL, Brady EM, McCann GP. Role of inflammation in diabetic cardiomyopathy. Ther Adv Endocrinol Metab. 2022;13:20420188221083530.
47. Jin L, Zhang J, Deng Z, Liu J, Han W, Chen G, et al. Mesenchymal stem cells ameliorate myocardial fibrosis in diabetic cardiomyopathy via the secretion of prostaglandin E2. Stem Cell Res Ther. 2020;11(1):122.
48. Wen HL, Liang ZS, Zhang R, Yang K. Anti-inflammatory effects of triptolide improve left ventricular function in a rat model of diabetic cardiomyopathy. Cardiovasc Diabetol. 2013;12:50.
49. Bryson TD, Gu X, Khalil RM, Khan S, Zhu L, Xu J, et al. Overexpression of prostaglandin E2, EP4 receptor improves cardiac function after myocardial infarction. J Mol Cell Cardiol. 2018;118:1-12.
50. Bosma KJ, Ghosh M, Andrei SR, Zhong L, Dunn JC, Ricciardi VF, et al. Pharmacological modulation of prostaglandin E2 (PGE2) EP receptors improves cardiomyocyte function under hyperglycemic conditions. Physiol Rep. 2022;10(7):e15212.
51. Mitrut R, Stepan AE, Pirici D. Histopathological aspects of the myocardium in dilated cardiomyopathy. Curr Health Sci J. 2018;44(3):243-249.
52. Singh R, Kaur N, Kishore L, Gupta GK. Management of diabetic complications: A chemical constituents-based approach. J Ethnopharmacol. 2013;150(1):51-70.
53. Khezri M, Rahbarghazi R, Ahmadi M, Sandoghchian S, Nourazarian A, Shademan B, et al. Type 2 Diabetes and its Effects on MicroRNA-155 and MicroRNA-133a Expression in Lung Tissue of Male Rats. J Clin Chem Lab Med. 2023;6(1):263.
54. Mazzon E, Cuzzocrea S. Role of TNF-α in lung tight junction alteration in mouse model of acute lung inflammation. Respir Res. 2007;8(1):75.
55. Zheng H, Wu J, Jin Z, Yan LJ. Potential biochemical mechanisms of lung injury in diabetes. Aging Dis. 2017;8(1):7-16.
56. Tomita Y, Fu Z, Wang Z, Cakir B, Cho SS, Britton W, et al. Long-acting FGF21 inhibits retinal vascular

leakage in in vivo and in vitro models. Int J Mol Sci. 2020;21(4):1188.
57. Das D, Shruthi NR, Banerjee A, Jothimani G, Duttaroy AK, Pathak S. Endothelial dysfunction, platelet hyperactivity, hypertension, and the metabolic syndrome: molecular insights and combating strategies. Front Nutr. 2023;10:1221438.
58. Babu V, Subathra Devi C. In vitro thrombolytic activity of purified streptokinase extracted from Streptococcus equinus VIT_VB2 isolated from bovine milk. J Thromb Thrombolysis. 2015;39(1):71-78.
59. Daryabor G, Atashzar MR, Kabelitz D, Meri S, Kalantar K. The effects of type 2 diabetes mellitus on organ metabolism and the immune system. Front Immunol. 2020;11:1582.
60. Zhang J, Deng Z, Jin L, Yang C, Liu J, Song H, et al. Spleen-derived anti-inflammatory cytokine IL-10 stimulated by adipose tissue-derived stem cells protects against type 2 diabetes. Stem Cells Dev. 2017;26(24):1749-1758.
61. Wang M, Xiong Y, Zhu W, Ruze R, Xu Q, Yan Z, et al. Sleeve gastrectomy ameliorates diabetes-related spleen damage by improving oxidative stress status in diabetic obese rats. Obes Surg. 2021;31(3):1183-1195.